NASA TECHNICAL MEMORANDUM

NASA TM X-2859

NASA TM X-2859

HEAT-TRANSFER CHARACTERISTICS OF A SINGLE CIRCULAR AIR JET IMPINGING ON A CONCAVE HEMISPHERICAL SHELL

by John N. B. Livingood and James W. Gauntner

Lewis Research Center

Cleveland, Ohio 44135

NATIONAL AERONAUTICS AND SPACE ADMINISTRATION • WASHINGTON, D. C. • AUGUST 1973

1. Report No.	2. Government Accession No.	3. Recipient's Catalog No.
NASA TM X-2859		

4. Title and Subtitle	5. Report Date
HEAT-TRANSFER CHARACTERISTICS OF A SINGLE CIRCULAR AIR JET IMPINGING ON A CONCAVE HEMISPHERICAL SHELL	August 1973
	6. Performing Organization Code

7. Author(s)	8. Performing Organization Report No.
John N. B. Livingood and James W. Gauntner	E-7462
	10. Work Unit No. 501-24

9. Performing Organization Name and Address	11. Contract or Grant No.
Lewis Research Center National Aeronautics and Space Administration Cleveland, Ohio 44135	
	13. Type of Report and Period Covered
12. Sponsoring Agency Name and Address	Technical Memorandum
National Aeronautics and Space Administration Washington, D.C. 20546	14. Sponsoring Agency Code

15. Supplementary Notes

16. Abstract

An experimental study was made of the local and average heat-transfer characteristics of a single turbulent air jet impinging on the concave surface of a hemisphere. Correlations were developed for expressing the effects of a number of dimensionless variables on the local and average Nusselt numbers. Results of the present study are compared with those from a similar study concerning a concave surface of a semicylindrical shell.

17. Key Words (Suggested by Author(s))	18. Distribution Statement
Impinging jet Concave hemispherical surface Heat-transfer data	Unclassified - unlimited

19. Security Classif. (of this report)	20. Security Classif. (of this page)	21. No. of Pages	22. Price*
Unclassified	Unclassified	15	$3.00

* For sale by the National Technical Information Service, Springfield, Virginia 22151

HEAT-TRANSFER CHARACTERISTICS OF A SINGLE CIRCULAR AIR JET IMPINGING ON A CONCAVE HEMISPHERICAL SHELL

by John N. B. Livingood and James W. Gauntner

Lewis Research Center

SUMMARY

An experimental study was made of the heat-transfer characteristics of a single turbulent air jet impinging on the concave surface of a hemispherical shell. Data were obtained for air jets of diameter 0.318, 0.635, and 0.952 centimeter (0.125, 0.250, and 0.375 in.), for nozzle-to-target separation distances of 3, 4, 5, 7, 10, and 14 nozzle diameters, and for nozzle- to hemisphere-diameter ratios of 0.0207, 0.0413, and 0.062. Reynolds numbers based on nozzle diameter and nozzle exit velocity ranged from 13 000 to 83 000.

Nusselt number correlations were obtained from local, stagnation-point, and average data. Both the data and the correlations are presented. When compared with the correlations, both the stagnation-point and average data are generally within ±10 percent.

A correlation for the ratio of local to average Nusselt number was also obtained and compared to a similar correlation for a semicylinder. The favorable comparison adds veracity to the semicylinder correlation, which can be used in the design of the leading-edge region of turbine vanes and blades.

INTRODUCTION

Experimentally determined heat-transfer characteristics for a single circular turbulent air jet impinging on a concave hemispherical surface are reported. Methods for correlating the stagnation-point, local, and average Nusselt numbers, and the ratio of local to average Nusselt numbers with geometrical parameters are presented.

An effective method of cooling the leading-edge region of turbine vanes and blades is by impingement of cool air on the internal surface. Reference 1 presents a review of the available literature on impingement on a concave cylindrical surface and some ex-

perimental average heat-transfer data. Reference 2 augments the results of reference 1 by presenting experimentally determined local to average Nusselt number ratio correlations as a function of dimensionless parameters.

This report presents empirical correlations for Nusselt numbers on the concave side of a hemispherical shell and compares one of these correlations with a similar correlation for a concave semicylindrical surface from reference 2. A favorable comparison between these correlations will further verify the correlation of reference 2, which is used in the design of the leading-edge region of turbine vanes and blades.

The data presented herein were obtained for a single circular air jet impinging on the concave surface of a hemispherical shell of inside diameter 15.36 centimeters (6.05 in.). Air jets of diameters 0.318, 0.635, and 0.952 centimeter (0.125, 0.25, and 0.375 in.) were considered with nozzle-to-target separation distances of 3, 4, 5, 7, 10, and 14 nozzle diameters. Reynolds numbers based on nozzle diameter and nozzle exit velocity ranged from 13 000 to 83 000.

The data were obtained under supervision of Dr. Peter Hrycak at the Newark College of Engineering under NASA Contract NAS3-11175.

SYMBOLS

A_{tot}	hemispherical surface area
A_x	cooled area along target measured from stagnation point
$a_0, \ldots, a_4$	correlation constants in eqs. (1), (2), (3), and (5)
B	exponent defined by eq. (5)
c_n	center-to-center nozzle separation distance
D	target diameter
d	nozzle diameter
$\dot{Nu}_0, \ldots, \dot{Nu}_5$	Nusselt numbers based on nozzle diameter related to calorimeter locations 0 to 5
$\dot{Nu}_x$	local Nusselt number based on nozzle diameter
$\overline{\dot{Nu}}$	average Nusselt number based on nozzle diameter
R	radius of target semicylinder
Re	Reynolds number based on nozzle diameter and nozzle exit velocity
z_n	nozzle-to-target separation distance

Subscripts:

cor correlated

exp experimental

APPARATUS

Heat-Transfer Surface

The concave side of a smooth ebonite hemispherical shell 15.36 centimeters (6.05 in.) in diameter and 1.83 centimeters (0.72 in.) thick formed the heat-transfer surface. Figure 1 shows this surface and the locations of 14 drilled holes in which calorimeters were placed to measure the heat flux. The ebonite shell and the calorimeters were secured tightly to a 0.13-centimeter- (0.05-in.-) thick brass hemispherical shell (fig. 1). Good thermal contact between the ebonite shell and the brass shell and between the calorimeters and the brass shell was achieved by introducing a thin layer of silver-loaded epoxy at the interface. The test shell was maintained at a constant temperature by condensing steam from a boiler on the convex side of the brass shell. The brass shell was attached to the boiler by means of a flange. A rubber gasket prevented steam leakage at the connecting joint.

Steam Boiler

A 25.4-centimeter- (10-in.-) long section of a steel pipe 24.13 centimeters (9.50 in.) in diameter was used to fabricate the boiler. The boiler, which was vented to atmosphere, was partially filled with water and was equipped with a wire mesh just above the water level to prevent splashing of the boiling water to the convex side of the brass hemispherical shell. A 110-volt, 1000-watt ac immersion heater whose power input was regulated by a 20-ampere variable transformer was used to heat the water. The boiler was placed in a square plywood box filled with fiber glass insulation to minimize heat losses. The complete assembly was supported on a triangular stand with three threaded legs to enable leveling and vertical adjustment of the nozzle-to-target separation distance.

Coolant Supply and Impingement Nozzles

Air supplied by a compressor flowed through a filter and oil separator into a large

storage tank to provide a steady flow. From the storage tank, the air flowed through an inlet tank connected to a set of four rotameters in parallel. Depending on the flow rate, the flow was routed through a selected rotameter and into a tube connected to a plenum chamber. The air then passed through a single circular impingement nozzle and impinged on the concave side of the hemispherical test surface. Nozzles of diameter 0.318, 0.635, and 0.952 centimeter (0.125, 0.25, and 0.375 in.) were investigated at nozzle-to-target separation distances, 3, 4, 5, 7, 10, and 14 nozzle diameters.

The rotameters were calibrated within an error of less than 1 percent of full scale. Air pressure was measured at the inlet of the rotameter with a Bourdon-type pressure gage with an assumed accuracy of ±0.34 newton per square centimeter (±0.50 psia). The inlet valve was kept fully open, and the flow was controlled by adjusting the outlet valve of the rotameter. The air temperature in the rotameter was measured by a thermocouple placed in the pipe.

Calorimeters

Fourteen 304-stainless-steel calorimeters embedded at locations on the test surface as shown in figure 1 were used to measure the heat flux. A sketch of the calorimeter is shown in figure 2. Each calorimeter was 0.953 centimeter (0.375 in.) in diameter and 1.827 centimeters (0.719 in.) long and contained two copper-constantan thermocouples along its axis; the thermocouples were located 0.140 centimeter (0.055 in.) from either end of the calorimeter. Each calorimeter was silver-soldered to a threaded bolt at the bottom and held in place on the surface by tightening a washer and nut. The calorimeters were enclosed in stainless-steel sleeves 1.11 centimeters (0.44 in.) in inside diameter and 0.16 centimeter (0.06 in.) thick, press fitted at the bottom to the brass plate. At the top, the small gap between the calorimeter and the sleeve was closed with nonconducting silicon rubber, thus creating an air pocket which formed an effective insulation against heat transfer from the calorimeter side wall.

Figure 1 shows provision for a single calorimeter at the stagnation point, two calorimeters at 11.5° on either side of the stagnation point, two more calorimeters at 22° on either side of the stagnation point, and single calorimeters 35.5°, 56°, and 80.5° from the stagnation point; these latter three calorimeters are also duplicated at angles of 120° and 240° from the line of the other calorimeters (fig. 1).

EXPERIMENTAL PROCEDURE

After a nozzle was selected and installed and a nozzle-to-target separation distance was set, the apparatus was leveled in the horizontal plane directly below the impinging

jet. The center stagnation point was made to coincide exactly with the axis of the impinging jet. The air jet was adjusted to the required Reynolds number, and a set of data was taken. Other Reynolds numbers were considered and were obtained by adjusting the outlet values of the rotameter, and other sets of data were taken.

The same procedure was followed for different nozzle-to-target separation distances and different nozzle diameters. A total of 62 sets of data were taken for the following conditions:

(1) Nozzle diameters - 0.318, 0.635, and 0.952 centimeter (0.125, 0.250, and 0.375 in.)

(2) Reynolds numbers - 13 000 to 88 000

(3) Nozzle-to-target separation distances - 3, 4, 5, 7, 10, and 14 nozzle diameters

Forty-seven of these 62 sets of data were for nozzle-to-target separation distances less than or equal to 7.

CORRELATION OF DATA

In order to correlate the heat-transfer data, the effects on Nusselt number of the dimensionless parameters Re, d/D, z_n/d, and A_x/A_{tot} must be investigated. (The last parameter is only required when local Nusselt numbers are considered.) Correlations were determined for local, stagnation-point, and average Nusselt numbers, and for the ratio of local to average Nusselt numbers by obtaining least-square curve fits of the data to the following equations:

Local:
$$Nu_x = a_0(Re)^{a_1}\left(\frac{d}{D}\right)^{a_2}\left(\frac{z_n}{d}\right)^{a_3}\left(\frac{A_x}{A_{tot}}\right)^{a_4} \tag{1}$$

Stagnation point:
$$Nu_0 = a_0(Re)^{a_1}\left(\frac{d}{D}\right)^{a_2}\left(\frac{z_n}{d}\right)^{a_3} \tag{2}$$

Average:
$$\overline{Nu} = a_0(Re)^{a_1}\left(\frac{d}{D}\right)^{a_2}\left(\frac{z_n}{d}\right)^{a_3} \tag{3}$$

Ratio of local to average:
$$\frac{Nu_x}{\overline{Nu}} = (B + 1)\left(\frac{A_x}{A_{tot}}\right)^{B} \tag{4}$$

where

$$B = a_0(Re)^{a_1}\left(\frac{d}{D}\right)^{a_2}\left(\frac{z_n}{d}\right)^{a_3} \tag{5}$$

Although the ratio of local to average Nusselt numbers can be obtained by taking the ratio of equation (1) to equation (2), the expression given by equation (4) is used herein so that a direct comparison can be made with the results of reference 2.

Since a separate correlation was obtained for the stagnation-point Nusselt number, the local Nusselt number correlation was limited to the five angular positions on the plate, distinct from the stagnation point, where heat-flux calorimeters were located (fig. 1(b)). The values of the local Nusselt numbers were obtained by averaging data for the several calorimeters of each angular position. In order to determine an average Nusselt number for the entire surface, it was necessary to determine weighting factors for each of the six local angularly spaced calorimeters. The weighting factors were calculated as the ratio of the area of shell segments to the area of the entire hemisphere. The weighting factors were found to be 0.0101, 0.0364, 0.0829, 0.1840, 0.3246, and 0.3621 for the calorimeter locations for the stagnation point and for successively larger angular positions, respectively.

RESULTS AND DISCUSSION

The data presented in table I were used in evaluating the coefficients and exponents of the dimensionless variables in equations (1), (2), (3), and (5). Maximum heat transfer for a jet impinging on a flat plate occurred when the nozzle-to-plate separation distance was 7 nozzle diameters. With the assumption that similar conditions apply to a jet impinging on a hemispherical surface, two sets of correlations were determined for the data presented herein: one set for the case where $z_n/d \leq 7$, and the other for the case where $z_n/d \geq 7$. Coefficients and exponents for equations (1), (2), (3), and (5) are given for both ranges of z_n/d in table II. However, the detailed discussion and graphical presentations of the stagnation-point, local, and average Nusselt numbers, and the ratio of local to average Nusselt numbers in the following sections are limited to the range of z_n/d values that are less than or equal to 7.

Local Nusselt Numbers

The correlation for the local Nusselt number for the case $z_n/d \leq 7$ was found to be

$$Nu_x = 2.04(Re)^{0.586}\left(\frac{d}{D}\right)^{1.10}\left(\frac{z_n}{d}\right)^{-0.023}\left(\frac{A_x}{A_{tot}}\right)^{-0.306} \tag{6}$$

considering the 235 local off-stagnation-point Nusselt numbers obtained from table I. Figure 3 compares the correlated and experimental local Nusselt numbers. The stagnation-point Nusselt numbers are not included in this correlation. The circles, squares, and triangles represent the three nozzle sizes 0.318, 0.635, and 0.925 centimeter (0.125, 0.250, and 0.375 in.), respectively. For the range of conditions considered, the figure shows most of the data are within about 10 percent of the correlated results. The constants and components for the cases $z_n/d \geq 7$ are given in table II.

Stagnation-Point Nusselt Numbers

The correlation equation for the stagnation-point Nusselt number for $z_n/d \leq 7$ was found to be

$$Nu_0 = 1.04(Re)^{0.554}\left(\frac{d}{D}\right)^{0.300}\left(\frac{z_n}{d}\right)^{0.004} \tag{7}$$

when all 47 sets of data were considered. Figure 4 compares the correlated and experimental stagnation-point Nusselt numbers. As in figure 3, the circles, squares, and triangles represent the three nozzle sizes in order of increasing diameter. For the range of conditions considered (three nozzle diameters, four nozzle-to-target separation distances, and a range of nozzle exit Reynolds numbers), the figure shows good agreement, generally about a ±10 percent variation around the 45° line.

Average Nusselt Numbers

A comparison of correlated and experimental average Nusselt numbers is presented in figure 5 for $z_n/d \leq 7$. The correlation equation for the average Nusselt numbers was found to be

$$\overline{Nu} = 2.98(Re)^{0.585}\left(\frac{d}{D}\right)^{1.10}\left(\frac{z_n}{d}\right)^{-0.007} \tag{8}$$

when all 47 sets of data were considered. The circles, squares, and triangles on the figure again represent the nozzles in order of increasing diameter. In general, figure 5 shows good agreement between the correlated and experimental values for all three nozzles sizes, four nozzle-to-target separation distances, and a range of nozzle exit Reynolds numbers. Generally, the data fall within ±10 percent around a 45° line.

Ratio of Local to Average Nusselt Numbers

The correlation equation for determining the ratio of local to average Nusselt numbers was found to be

$$\frac{Nu_x}{\overline{Nu}} = (B + 1)\left(\frac{A_x}{A_{tot}}\right)^B \tag{9}$$

where

$$B = -0.143(Re)^{0.023}\left(\frac{d}{D}\right)^{-0.221}\left(\frac{z_n}{d}\right)^{-0.146} \tag{10}$$

as determined from a least-squares curve fit of all data except stagnation-point data for $z_n/d \leq 7$. Figure 6 shows a comparison of the correlated and experimental results. The circles, squares, and triangles again represent the nozzles in order of increasing diameter.

Local values of Nusselt number can also be obtained by combining correlation (9) with the correlation for average Nusselt number.

Comparison Between Correlations for Hemisphere and Semicylinder

Figure 7 compares the ratio of local to average Nusselt numbers for a hemisphere with that for a semicylinder. The correlations used in this comparison are equations (9) and (10) of this report and equation (5) of reference 2. Values of dimensionless parameters z_n/d, d/D, and Re used to evaluate the correlations are taken from reference 3, which presents impingement data from a cooled turbine blade. In order that the semicylinder and hemisphere both of equal diameter have the same cooled area, the ratio of the center-to-center nozzle spacing to semicylinder diameter c_n/D must equal unity. (Area of semicylinder/area of hemisphere = $\pi R c_n / 2\pi R^2 = c_n/2R = c_n/D = 1.$)

The distributions shown in figure 7 are similar over the entire range, having a maximum deviation of slightly over 2 percent at the extremes of the curve. At large values of the abscissa, the ratio of local to average Nusselt numbers is lower for the hemisphere than for the semicylinder.

The agreement between these correlations, when evaluated with dimensionless parameters typical of a turbine blade, lends support to the correlation given in reference 2. With this added support the designer can have more confidence when using this correlation in the design of the leading-edge region of turbine vanes and blades.

SUMMARY OF RESULTS

The results of an experimental study of the heat-transfer characteristics of a single turbulent air jet impinging on the concave surface of a hemisphere are as follows:

1. Correlations are presented for local, stagnation-point, and average Nusselt numbers, and for the ratio of local to average Nusselt numbers. In general, the correlations and the data agree within about 10 percent.

2. This ratio-of-local-to-average-Nusselt-number correlation compares favorably with a similar correlation for the concave surface of a semicylindrical shell. Such a favorable comparison substantiates the semicylinder correlation which is used in the design of turbine vanes and blades.

Lewis Research Center,
National Aeronautics and Space Administration,
Cleveland, Ohio, May 18, 1973,
501-24.

REFERENCES

1. Livingood, John N. B.; and Gauntner, James W.: Average Heat-Transfer Characteristics of a Row of Circular Air Jets Impinging on a Concave Surface. NASA TM X-2657, 1972.

2. Livingood, John N. B.; and Gauntner, James W.: Local Heat-Transfer Characteristics of a Row of Circular Air Jets Impinging on a Concave Semicylindrical Surface. NASA TN D-7127, 1973.

3. Gauntner, James W.; and Livingood, John N. B.: Engine Investigation of an Impingement-Cooled Turbine Rotor Blade. NASA TM X-2791, 1973.

TABLE I. - HEAT-TRANSFER DATA

Ratio of nozzle to target diameter, d/D	Average Nusselt number, $\overline{Nu}$	Ratio of nozzle-to-target separation distance to nozzle diameter, z_n/d	Reynolds number, Re	Local to average Nusselt number ratio for calorimeter locations 0 to 5					
				$\frac{Nu_5}{\overline{Nu}}$	$\frac{Nu_4}{\overline{Nu}}$	$\frac{Nu_3}{\overline{Nu}}$	$\frac{Nu_2}{\overline{Nu}}$	$\frac{Nu_1}{\overline{Nu}}$	$\frac{Nu_0}{\overline{Nu}}$
0.0207	10.69	3	13 770	0.721	0.852	1.097	1.308	2.536	5.922
	16.29	3	26 000	.729	.828	1.086	1.369	2.648	5.713
	25.00	3	54 410	.716	.811	1.088	1.413	2.723	6.060
	28.93	3	66 270	.720	.808	1.092	1.410	2.678	6.210
	10.88	4	14 250	.681	.860	1.151	1.387	2.540	5.444
	17.31	4	27 580	.729	.838	1.115	1.375	2.538	5.188
	24.69	4	55 240	.671	.817	1.124	1.595	2.616	5.690
	27.73	4	69 920	.708	.821	1.122	1.474	2.585	5.378
	10.70	5	14 870	.683	.875	1.121	1.370	2.284	5.413
	16.52	5	27 440	.697	.852	1.112	1.413	2.619	5.361
	24.59	5	55 250	.699	.828	1.127	1.425	2.598	5.735
	29.05	5	69 070	.734	.817	1.101	1.424	2.583	5.459
	11.14	7	14 460	.717	.870	1.136	1.286	2.449	5.271
	16.94	7	27 290	.732	.854	1.097	1.332	2.549	5.208
	25.24	7	55 660	.874	.648	1.158	1.375	2.550	5.273
	27.02	7	85 780	.708	.829	1.113	1.435	2.646	5.405
	23.12	14	13 360	.781	.984	1.176	1.169	1.652	2.417
	36.29	14	25 830	.740	1.000	1.195	1.184	1.802	2.363
0.0413	36.80	3	25 760	0.737	0.842	1.150	1.478	2.586	3.122
	59.97	3	55 540	.753	.826	1.145	1.485	2.629	2.918
	51.52	3	74 470	.971	.605	.613	2.016	3.610	3.997
	25.10	4	14 250	.711	.858	1.179	1.443	2.517	3.575
	37.17	4	26 840	.724	.872	1.171	1.424	2.443	3.209
	58.49	4	56 870	.737	.850	1.168	1.442	2.520	3.087
	59.77	4	70 400	.805	.932	1.300	.357	2.822	3.408
	23.41	5	13 530	.729	.881	1.172	1.382	2.313	3.537
	35.66	5	27 000	.728	.862	1.178	1.428	2.399	3.377
	56.06	5	57 106	.720	.863	1.178	1.460	2.428	3.253
	66.84	5	74 890	.729	.846	1.179	1.470	2.481	3.179
	22.00	7	13 320	.679	.907	1.222	1.427	2.222	3.549
	34.82	7	26 470	.700	.898	1.192	1.442	2.264	3.397
	55.26	7	56 560	.712	.876	1.207	1.467	2.241	3.213
	62.74	7	71 390	712	.881	1.205	1.464	2.234	3.170
	25.63	10	13 500	.745	.991	1.219	1.059	1.862	2.854
	37.75	10	26 140	.780	.938	1.121	1.241	2.034	2.923
	60.22	10	57 530	.736	.982	1.106	1.346	1.942	2.865
	66.88	10	71 150	.740	.910	1.194	1.413	1.957	2.844
	57.51	14	53 590	.758	.951	1.212	1.330	1.712	2.100
	58.24	14	67 870	.775	1.080	1.366	.286	1.879	2.528
0.0620	38.06	3	15 590	0.783	0.819	1.232	1.448	2.167	2.455
	60.01	3	30 770	.752	.882	1.201	1.443	2.158	2.179
	87.30	3	59 440	.760	.867	1.194	1.492	2.187	2.017
	104.72	3	83 830	.740	.880	1.205	1.501	2.207	1.970
	39.96	4	15 990	.750	.906	1.194	1.411	2.012	2.416
	60.35	4	31 020	.742	.900	1.193	1.455	2.094	2.264
	87.41	4	61 320	.735	.894	1.203	1.476	2.149	2.160
	99.16	4	78 270	.749	.883	1.197	1.475	2.148	2.114
	39.63	5	15 990	.771	.892	1.215	1.354	1.943	2.462
	60.64	5	32 050	.778	.894	1.160	1.414	2.024	2.350
	88.16	5	61 940	.764	.882	1.238	1.382	1.987	2.216
	99.67	5	78 920	.787	.892	1.166	1.384	2.030	2.196
	40.07	7	16 080	.748	.934	1.207	1.331	1.862	2.555
	62.72	7	31 720	.788	.905	1.183	1.344	1.854	2.402
	89.26	7	61 340	.784	.902	1.180	1.373	1.877	2.364
	101.09	7	88 140	.770	.949	1.071	1.434	1.985	2.466
	44.78	10	16 300	.809	.990	1.150	1.192	1.536	1.901
	58.60	10	30 000	.787	.947	1.191	1.249	1.708	2.227
	86.70	10	62 550	.787	.940	1.191	1.287	1.709	2.161
	84.27	10	78 740	.504	1.074	1.365	1.475	1.952	2.446
	40.20	14	15 850	.860	.970	1.129	1.137	1.469	1.819
	58.99	14	60 850	.871	.967	1.124	1.139	1.429	1.721
	65.95	14	62 250	.861	1.230	.433	1.473	1.803	2.125

TABLE II. - CONSTANTS AND EXPONENTS IN CORRELATION EQUATIONS

(a) Ratio of nozzle-to-target separation to nozzle diameter, z_n, ≤ 7

Equation	Equation for-	Constants and exponents				
		a_0(constant)	a_1(exp of Re)	a_2(exp of d/D)	a_3(exp of z_n/d)	a_4(exp of A_x/A_{tot})
(1)	Nu_x	2.04	0.586	1.10	-0.023	-0.306
(2)	Nu_0	1.04	.554	.300	.004	------
(3)	$\overline{Nu}$	2.98	.585	1.10	-.007	------
(5)	B	-.143	.023	-.221	-.146	------

(b) Ratio of nozzle-to-target separation distance to nozzle diameter, z_n, ≥ 7

Equation	Equation for-	Constants and exponents				
		a_0(constant	a_1(exp Re)	a_2(exp of d/D)	a_3(exp of z_n/d)	a_4(exp of A_x/A_{tot})
(1)	Nu_x	2.16	0.475	0.788	0.107	-0.237
(2)	Nu_0	3.15	.519	.275	-.407	------
(3)	$\overline{Nu}$	2.22	.477	.804	.238	------
(5)	B	-.405	.052	-.245	-.857	------

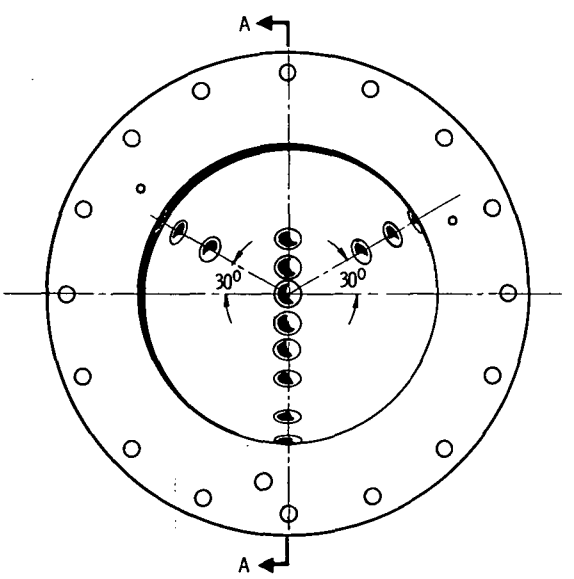

(a) Planar view.

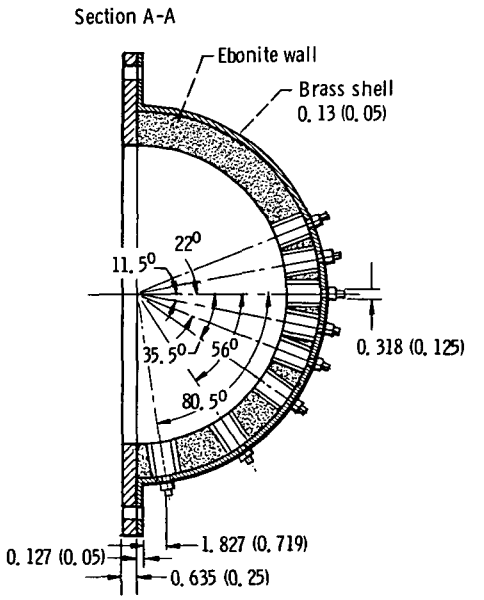

(b) Angular positions as measured from jet centerline. (Dimensions are in cm (in.).)

Figure 1. - Calorimeter positions in concave hemispherical shell.

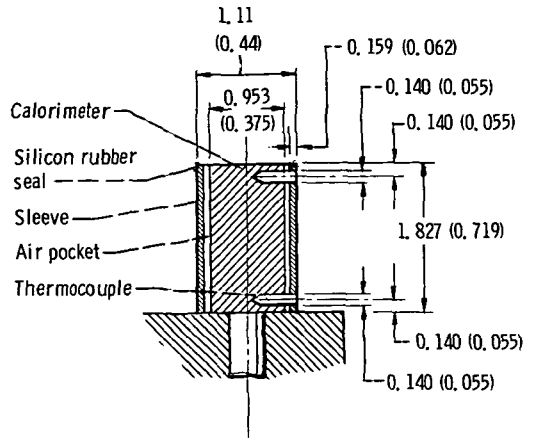

Figure 2. - Calorimeter used to measure heat flux. (Dimensions are in cm (in.).)

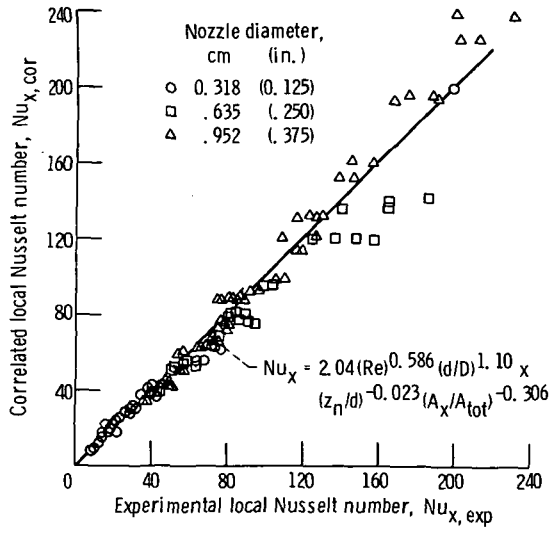

Figure 3. - Comparison between local Nusselt numbers on concave surface of 15.36-centimeter- (6.05-in.-) diameter hemispherical shell calculated from correlation and from data.

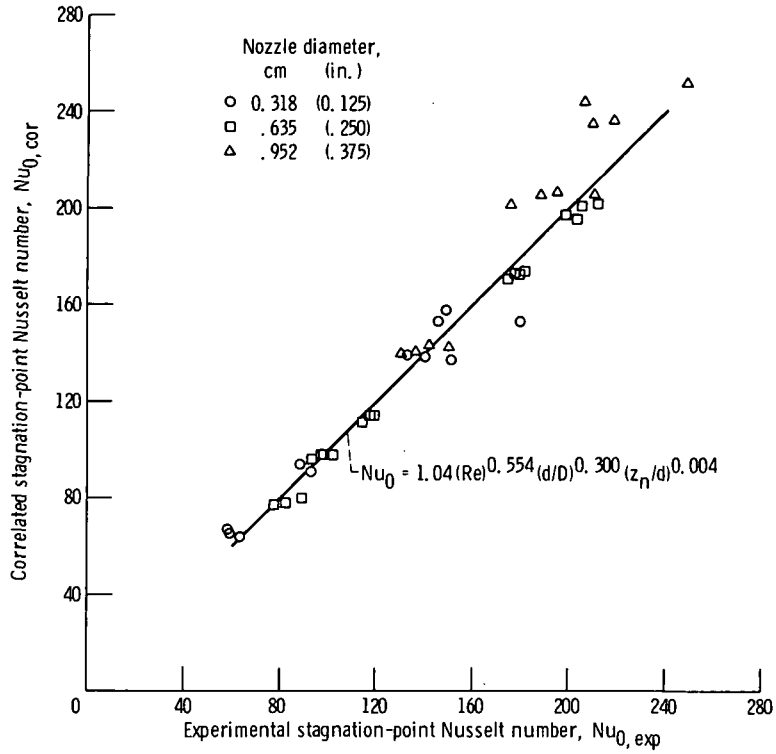

Figure 4. - Comparison between stagnation-point Nusselt numbers on concave surface of 15.36-centimeter- (6.05-in.-) diameter hemispherical shell calculated from correlation and from data.

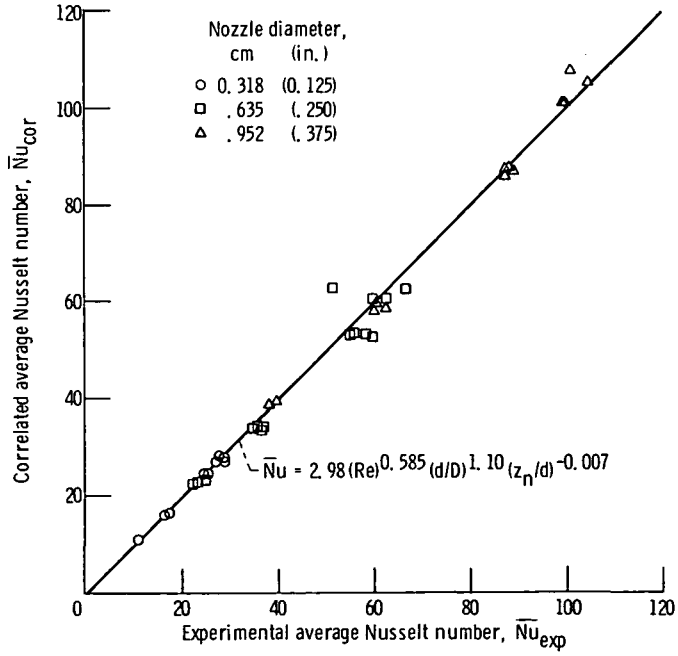

Figure 5. - Comparison between average Nusselt numbers over concave surface of 15.36-centimeter- (6.05-in.-) diameter shell calculated from correlation and from data.

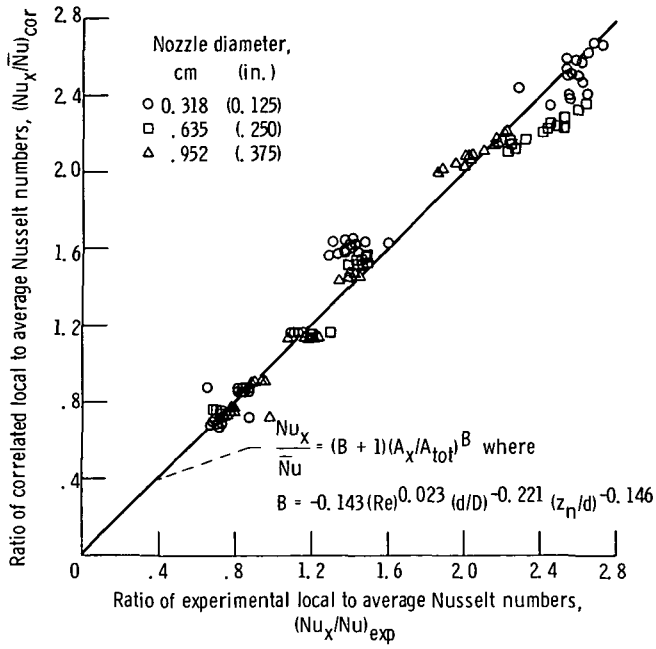

Figure 6. - Comparison between ratios of local to average Nusselt number on concave surface of 15.36-centimeter- (6.05-in.-) diameter hemispherical shell calculated from correlation and from data.

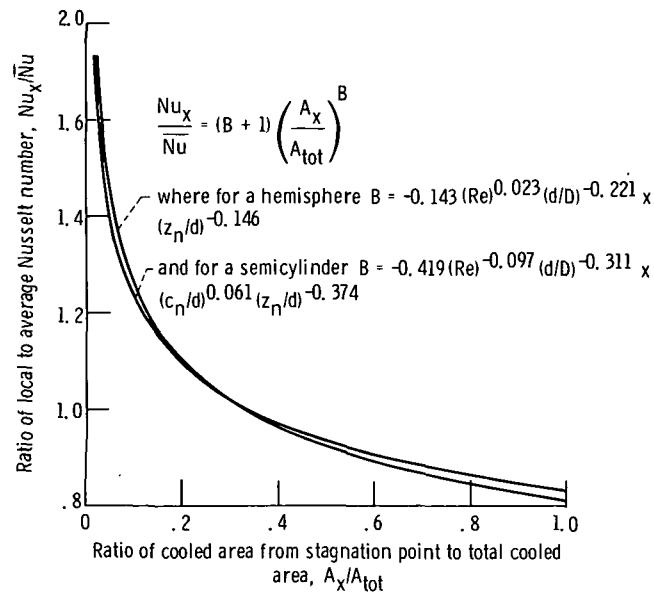

Figure 7. - Comparison between Nusselt number ratio distribution for a hemisphere with that for a semicylinder. Reynolds number, 5000; ratio of nozzle diameter to hemisphere diameter, 0.25; dimensionless nozzle-to-ta target separation distance, 5; dimensionless center-to-center nozzle spacing, 4.

NATIONAL AERONAUTICS AND SPACE ADMINISTRATION
WASHINGTON, D.C. 20546

OFFICIAL BUSINESS
PENALTY FOR PRIVATE USE $300

SPECIAL FOURTH-CLASS RATE BOOK

POSTAGE AND FEES PAID
NATIONAL AERONAUTICS AND SPACE ADMINISTRATION
451

U.S.MAIL

POSTMASTER: If Undeliverable (Section 158 Postal Manual) Do Not Return

"The aeronautical and space activities of the United States shall be conducted so as to contribute . . . to the expansion of human knowledge of phenomena in the atmosphere and space. The Administration shall provide for the widest practicable and appropriate dissemination of information concerning its activities and the results thereof."

—NATIONAL AERONAUTICS AND SPACE ACT OF 1958

NASA SCIENTIFIC AND TECHNICAL PUBLICATIONS

TECHNICAL REPORTS: Scientific and technical information considered important, complete, and a lasting contribution to existing knowledge.

TECHNICAL NOTES: Information less broad in scope but nevertheless of importance as a contribution to existing knowledge.

TECHNICAL MEMORANDUMS: Information receiving limited distribution because of preliminary data, security classification, or other reasons. Also includes conference proceedings with either limited or unlimited distribution.

CONTRACTOR REPORTS: Scientific and technical information generated under a NASA contract or grant and considered an important contribution to existing knowledge.

TECHNICAL TRANSLATIONS: Information published in a foreign language considered to merit NASA distribution in English.

SPECIAL PUBLICATIONS: Information derived from or of value to NASA activities. Publications include final reports of major projects, monographs, data compilations, handbooks, sourcebooks, and special bibliographies.

TECHNOLOGY UTILIZATION PUBLICATIONS: Information on technology used by NASA that may be of particular interest in commercial and other non-aerospace applications. Publications include Tech Briefs, Technology Utilization Reports and Technology Surveys.

Details on the availability of these publications may be obtained from:

SCIENTIFIC AND TECHNICAL INFORMATION OFFICE

NATIONAL AERONAUTICS AND SPACE ADMINISTRATION

Washington, D.C. 20546